minerals

MDPI

Article

Temperature-Induced Desorption of Methyl *tert*-Butyl Ether Confined on ZSM-5: An In Situ Synchrotron XRD Powder Diffraction Study

Elisa Rodeghero [1,*], Luisa Pasti [2], Elena Sarti [2], Giuseppe Cruciani [1], Roberto Bagatin [3] and Annalisa Martucci [1]

1 Department of Physics and Earth Sciences, University of Ferrara, Via Saragat 1, 44122 Ferrara (FE), Italy; giuseppe.cruciani@unife.it (G.C.); annalisa.martucci@unife.it (A.M.)
2 Department of Chemical and Pharmaceutical Sciences, University of Ferrara, Via Fossato di Mortara 17, 44121 Ferrara (FE), Italy; luisa.pasti@unife.it (L.P.); elena.sarti@unife.it (E.S.)
3 Research Centre for Non-Conventional Energy–Istituto Eni Donegani Environmental Technologies, Via Felice Maritano, 26, 20097 San Donato Milanese (MI), Italy; roberto.bagatin@eni.com
* Correspondence: elisa.rodeghero@unife.it or rdglse@unife.it; Tel.: +39-532-974730

Academic Editor: Peng Yuan
Received: 29 December 2016; Accepted: 16 February 2017; Published: 28 February 2017

Abstract: The temperature-induced desorption of methyl *tert*-butyl ether (MTBE) from aqueous solutions onto hydrophobic ZSM-5 was studied by in situ synchrotron powder diffraction and chromatographic techniques. This kind of information is crucial for designing and optimizing the regeneration treatment of such zeolite. The evolution of the structural features monitored by full profile Rietveld refinements revealed that a monoclinic ($P2_1/n$) to orthorhombic ($Pnma$) phase transition occurred at about 100 °C. The MTBE desorption process caused a remarkable change in the unit-cell parameters. Complete MTBE desorption was achieved upon heating at about 250 °C. Rietveld analysis demonstrated that the desorption process occurred without any significant zeolite crystallinity loss, but with slight deformations in the channel apertures.

Keywords: MTBE; ZSM-5; desorption; in situ synchrotron powder diffraction

1. Introduction

The removal of methyl-*tert*-butyl-ether (MTBE, $C_5H_{12}O$) from surface waters, groundwater and urban storm water is an important goal in water treatment technology [1,2] due to the widespread occurrence of MTBE, combined with possible human carcinogenic effects [3]. This chemical is one of the main constituents of petroleum fuel and is characterized by small molecular size, high aqueous solubility (43,000–54,300 mg·L^{-1}), low Henry's law constant (0.023–0.12; dimensionless), low vapour pressure (43 mg·L^{-1} and 249 mmHg at 25 °C), and high resistance to biodegradation [4,5]. The US Environmental Protection Agency (EPA) estimated that MTBE concentration in drinking water should not exceed 20 µg·L^{-1} in terms of odour and 40 µg·L^{-1} in terms of taste [6]. Currently, water treatment technologies, such as air stripping, aerobic biodegradation, filtration, chemical oxidation reactions and membrane technology involve high operation costs and could produce toxic secondary pollutants in the environment [1,7].

Recently, adsorption on hydrophobic zeolites has received the greatest interest in water treatment technology due to their organic contaminant selectivity, thermal and chemical stability, strong mechanical properties, rapid kinetics and absence of salt and humic substance interference [8–20]. In order for the adsorption process to be cost effective, the progressive deactivation of saturated sorbents has become an essential task [20]. Thermal treatment is the most common regeneration

technique, where organic host molecules are decomposed and/or oxidized at high temperature. Zeolites showed an excellent stability during the heating process and their behavior can be affected by several factors such as chemical composition, framework order-disorder and topology, nature and amount of extra-framework species, synthesis conditions, structure directing agents [21–28]. Consequently there is a strong interest in understanding the mechanisms behind the thermal regenerative solution which makes zeolites regenerable materials that are efficiently reusable in the contaminants adsorption process.

Several recent studies have demonstrated that zeolites exhibit considerably large MTBE adsorption uptakes [29–35] and that ZSM-5 was a cost-competitive adsorbent when considering both life time and usage rate of the adsorbent material [14,31]. Zeolite Socony Mobil-5 (ZSM-5, MFI-type framework topology [36]) is a medium pore material whose framework is characterized by two channel systems: sinusoidal 10-membered rings (10-MR) channels (ZZ) (sinusoidal ring A and sinusoidal ring B) along the (100) direction, interconnected with 10-MR straight channels (SC) (SC ring A and SC ring B) parallel to the (010) direction. Another tortuous pore path runs parallel to the (001) direction. The adsorption of MTBE onto high silica ZSM-5 zeolite (SiO_2/Al_2O_3 = 200) was investigated by Martucci et al. [31] by batch adsorption and X-ray powder diffraction (XRPD) analyses from aqueous solution, and by infrared spectroscopy from the gas phase in the presence of water. MTBE exhibits a type-I isotherm, thus indicating a different interaction mechanism. XRPD and infrared (IR) spectroscopy reveal the occurrence clustering of water and MTBE during adsorption from both the liquid and gas phase. These H-bonded oligomers interact with zeolite thus leading to framework flexibility for MFI-type zeolites. Rapid kinetics combined with good adsorption capacity suggest that this microporous material can be used to efficiently remove this emerging organic contaminant from water.

One of the main targets of the present work is to continuously monitor the thermal MTBE decomposition process, as well as the structural modifications on ZSM-5 upon temperature-programmed desorption treatment. This in situ synchrotron XRD powder diffraction study was used as a key to understand the features of both adsorption and desorption processes, thus helping in the design of water treatment appliances based on microporous materials.

2. Materials and Methods

2.1. Chemicals

Methyl *tert*-butyl ether (99% purity) and sodium chloride was obtained from Sigma-Aldrich (St. Louis, MO, USA). The concentration of contaminant in the aqueous solution was determined by Headspace Gas Chromatography coupled to Mass Spectrometry (HS-GC-MS). The ZSM-5 sample used in this work was a hydrophobic zeolite (code CBV 28014) provided by Zeolyst International (Conshohocken, PA, USA) in its ammonium form and used as received (SiO_2/Al_2O_3 molar ratio = 280, Na_2O < 0.05 wt % and surface area = 400 $m^2 \cdot g^{-1}$).

2.2. Experimental

The saturation capacity was determined using the batch method. Batch experiments were carried out in triplicate in 20 mL crimp top reaction glass flasks sealed with polytetrafluoroethylene (PTFE) septa (Supelco, Bellefonte, PA, USA). The flasks were filled in order to have the minimum headspace and a solid/solution ratio of 1:2 ($mg \cdot mL^{-1}$) was employed. After equilibration, for 24 h at a temperature of 25.3 ± 0.5 °C under stirring, the solids were separated from the aqueous solution by centrifugation (10,000 rpm for 30 min) and analysed by HS-SPME-GC. More details are reported in Martucci et al. [31]. The MTBE adsorbed quantities (q) and equilibrium concentrations (Ce), were determined in solution before and after equilibration with the zeolite by HS-SPME-GC.

2.3. Instrumentation

The analysis was carried out using an Agilent GC-MS system (Santa Clara, CA, USA) consisting of a GC 6850 Series II Network coupled to a Pal G6500-CTC injector and a Mass Selective Detector 5973 Network. The injected solutions consist of 100 mL of sample solutions, diluted in 10 mL of an aqueous solution saturated with NaCl, containing 10 mL of 500 mg·L^{-1} of fuorobenzene in methanol as the internal standard. HS autosampler injector conditions are as follows: incubation oven temperature 80 °C, incubation time 50 min, headspace syringe temperature 85 °C, agitation speed 250 rpm, agitation on time 30 s, agitation off time 5 s, injection volume 500 mL. In situ high-temperature X-ray diffraction data were collected at the high-resolution powder diffraction beamline ID31 (European Synchrotron Radiation Facility, ESRF, Grenoble, France). Once diffracted, the incident X-ray (λ = 0.400031 Å) was directed through nine Si 111 analyzer crystals and then collected in parallel by means of nine detectors. A subsequent data-reduction was performed to produce the equivalent step scan. X-ray diffraction patterns were recorded from room temperature to 600 °C in air (heating rate of 0.083 °C·s^{-1}), in the 0.5–19.5 2θ range. The General Structure Analysis System (GSAS) [37] package with the Experiment Graphical User Interfaces (EXPGUI) graphical interface [38] was used for Rietveld structure refinements starting from the framework fractional atomic coordinates reported by Martucci et al. [31]. The typical Rietveld fits from the temperature series and a table of the R*wp* at all temperatures are reported as Supplementary Materials (Figures S1–S17). Atomic coordinates at 30, 100 and 400 °C are also reported as Supplementary Materials (Tables S1–S3).

3. Results and Discussion

3.1. Adsorption from Aqueous Solutions

MTBE adsorption isotherms on ZSM-5 were obtained at 25 °C by Martucci et al. [31] and follow a Langmuir model. This indicates that the interactions of MTBE with the zeolite framework are energetically similar to each other. Starting from the isotherm data, saturated samples were prepared by putting into contact a given amount of zeolite with an aqueous solution of MTBE having a concentration of 200 mg·L^{-1}. The adsorbed quantity q (mg·g^{-1}) was calculated as follows:

$$q = \frac{(C_0 - C_e)V}{m} \quad (1)$$

where C_0 is the initial concentration in solution (mg·L^{-1}), C_e is the concentration at equilibrium (mg·L^{-1}), V is the solution volume (L) and m is the mass of sorbent (g). Four different samples were prepared, the average saturation capacity and standard deviation were 95 ± 7 mg·g^{-1}, confirming the saturation capacity previously found in Martucci et al. [31]. The saturated samples were homogenized and employed for the structural analysis.

After thermal desorption, the three samples of regenerated zeolite were saturated with MTBE in the same conditions. The average saturation capacity was 92 ± 8 mg·g^{-1}. Therefore, the regenerated material shows an adsorption capacity that does not significantly differ from that of the as received materials, confirming the possibility to reuse the adsorbent material.

3.2. Structural Analyses

According to Martucci et al. [31], MTBE molecules are hosted in two crystallographically independent sites: MTBE1 near the intersections of sinusoidal and straight 10 MR channels (C1a, C2a, C3a, C4a, C5a, O1a sites in Table S1); and MTBE2 in the sinusoidal 10 MR channel (C1b, C2b, C3b, C4b, C5b, O1b sites in Table S1), respectively. Figure 1 shows the high-loaded structure of ZSM-5-MTBE, with the guest molecules located in both channels. On the whole, eight MTBE molecules (corresponding to ~11% zeolite dry weight (dw)) and about two water molecules (corresponding to about 0.5% zeolite dw) were detected. Rietveld structure refinement confirmed the occurrence of

MTBE–water complexes interacting with the framework, stabilizing the guest structure within the zeolite host framework. The presence of organic compound–water molecule oligomers has also been recently reported in mordenite [39], ferrierite [29] as well as in the same Y and ZSM-5 zeolite after 1,2-dichloroethane (DCE) adsorption from aqueous solutions [18].

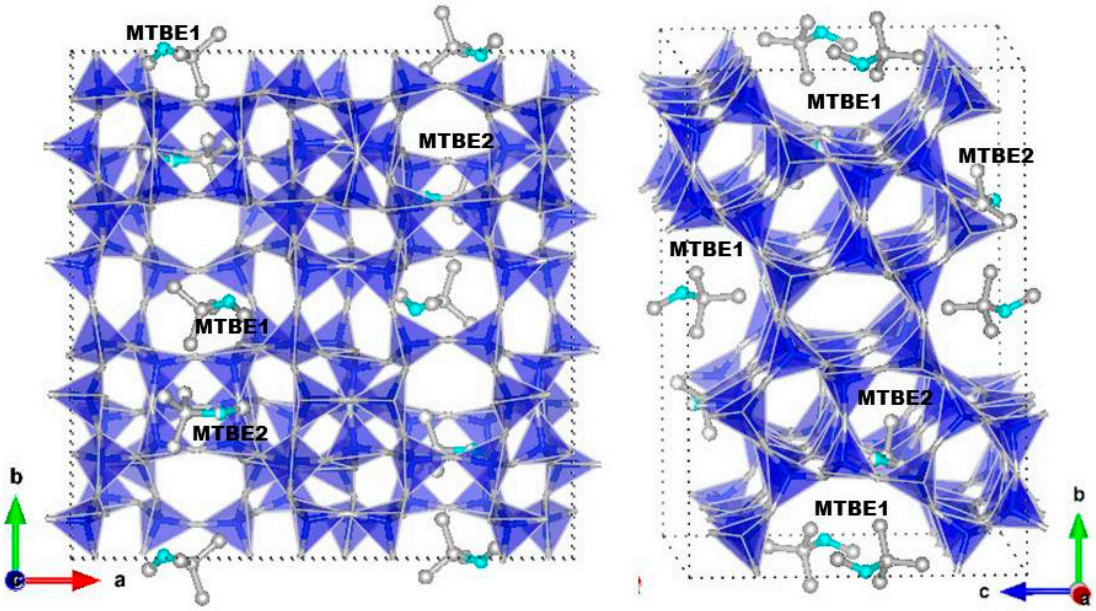

Figure 1. High-loaded structure of ZSM-5-methyl-*tert*-buthyl-ether (MTBE) along *a* and *c* directions, respectively. Water molecules are represented as light blue spheres.

The automatic indexing of the peaks, carried out by the High Score Plus v. 3.0 software [40], revealed the gradual overlapping of groups of peaks (i.e., 131 + 13 − 1 and 311 + 31 − 1 in the first angular range, and 133 + 13 − 3 and 313 + 31 − 3 in the second range) attesting the monoclinic to orthorhombic phase transition, with a Tc close to 100 ± 5 °C. Figure 2 shows the evolution of the investigated ZSM-5 sample close to the expected transition temperature, Tc, in the 3.70–4.30 and 5.60–6.50 2θ range. Therefore, recent works [41–43] reported this phenomenon both in the unloaded ZSM-5 as well as in the same samples after organics adsorption. The evolution of refined unit cell parameters as a function of temperature is illustrated in Figure 2.

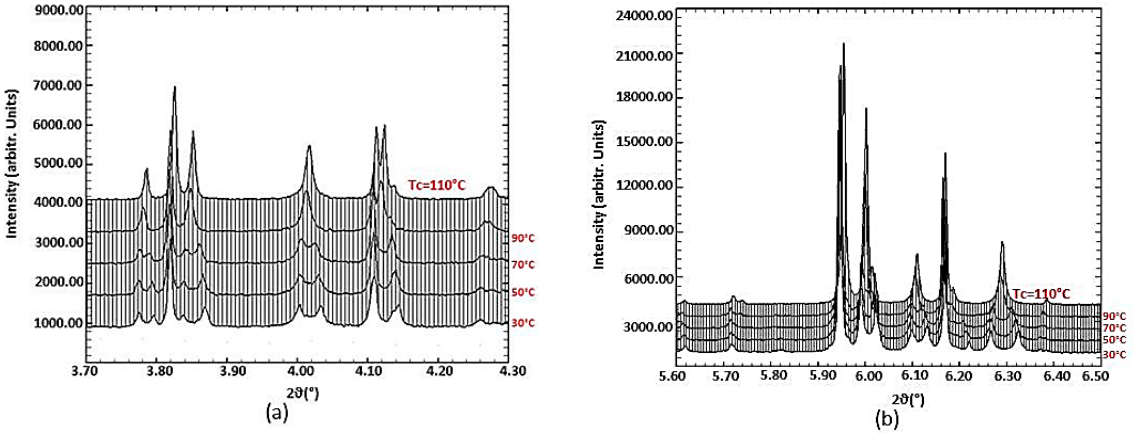

Figure 2. Evolution of the investigated ZSM-5-MTBE close to the expected transition temperature (30, 50, 70, 90 and 110 °C, respectively) in the 3.70–4.30 (**a**) and 5.60–6.50 (**b**) 2θ (°) range.

The general trend shows an initial increase of all the lattice parameters except for the b parameter (Figure 3 and Table S1). In particular, the unit cell volume increases until about 125 ± 5 °C, then it remains about constant in the range between 125 and 200 ± 5 °C and starts to decrease after 200 ± 5 °C. Similar behaviour was observed during the desorption process of 1,2-dichloroethane [44] and toluene [45].

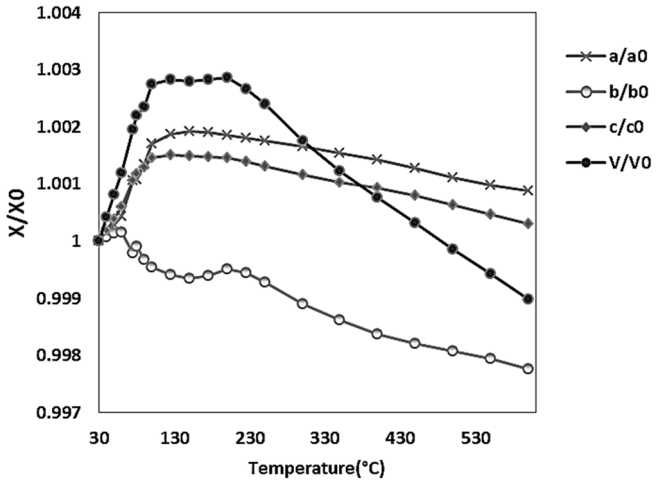

Figure 3. Temperature evolution of ZSM-5-MTBE unit cell parameters during in situ thermal organic burning. All values are normalized compared to those refined at room temperature.

According to Pasti et al., Martucci et al. [44] and Rodeghero et al. [45] this behavior can be explained by the relaxation of the interactions between the oligomers and the framework oxygens. The refined distances clearly indicate that during the heating, this attractive force exerting a negative pressure is released and the framework is free to relax and expand. The process is also correlated to the MTBE desorption process which starts at 100 °C and is complete at ~300 °C. Figure 4 shows both the evolution of MTBE molecules per unit cell (p.u.c.) and the unit cell volume as a function of temperature.

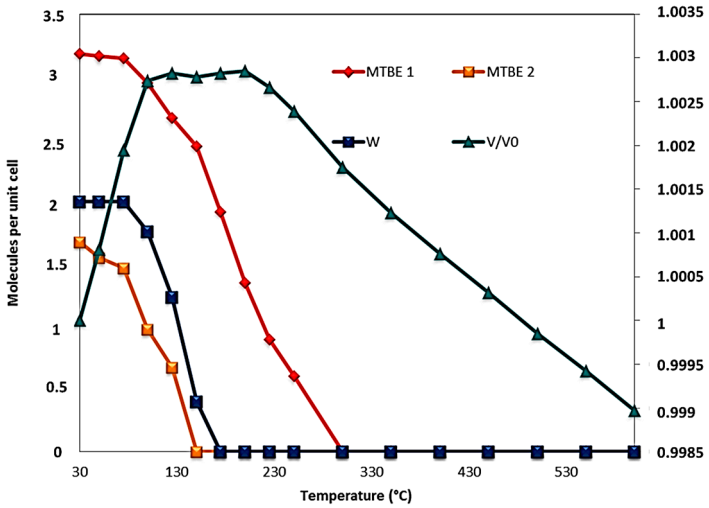

Figure 4. Evolution of MTBE and water (W) molecules and unit cell volume as a function of temperature.

After the full desorption of organics, a contraction of the unit cell volume is observed until 600 °C. This phenomenon is explained as a thermal negative expansion (NTE), already observed not

only in MFI-type materials [41,45–48], but also in other microporous materials [22–27,48–51], thus attesting the relaxation of framework distortions induced by host molecules which diffuse through the zeolite channels during the heating process. The desorption process occurred without any significant zeolite crystal. Above 300 °C, the channels ellipticity decreases and wide-open apertures regularize. This process is accompanied by variations in the opening of the zeolite framework pore system and consequently, in the Crystallographic Free Areas (C.F.A.) (Figure 5).

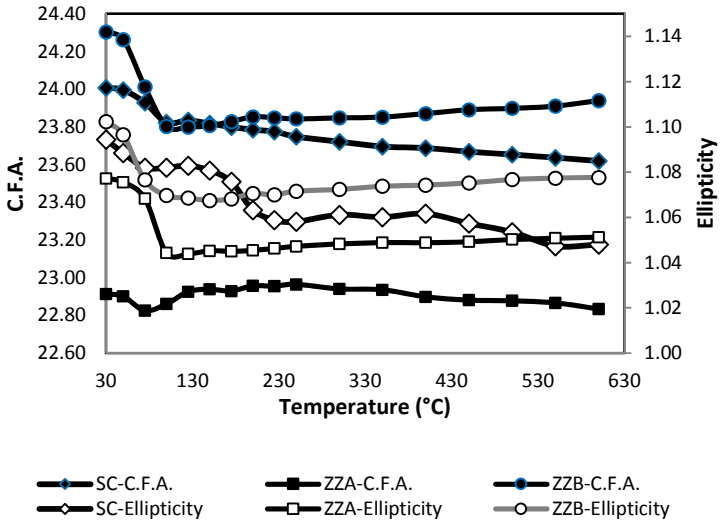

Figure 5. Crystallographic Free Areas (C.F.A.) of the 10-ring channels and ellipticity of the 10-ring channels as a function of temperature. ZZ stands for zigzag or sinusoidal channel; SC stands for straight channel.

4. Conclusions

This study reports experimental results concerning the desorption of methyl-*tert*-butyl-ether from the pores of a silica-rich zeolite ZSM-5. The temperature-induced desorption of this oxygenated compound from aqueous solutions onto hydrophobic ZSM-5 was studied by combining in situ synchrotron powder diffraction and chromatographic techniques. The evolution of the structural features monitored by full profile Rietveld refinements revealed that a monoclinic ($P2_1/n$) to orthorhombic (P*nma*) phase transition occurred at about 100 °C. Complete MTBE desorption was achieved upon heating at about 250 °C. Notwithstanding the change in the unit-cell parameters, Rietveld refinement demonstrated that the desorption process occurred without any significant zeolite crystallinity loss, but with slight deformations in the channel apertures. After the full organics desorption, a contraction of the unit cell volume is observed, thus indicating negative thermal expansion (NTE) for this material. On the basis of all these results, ZSM-5 represents a promising adsorbent medium to remove MTBE contaminant from water.

Supplementary Materials: The following are available online at www.mdpi.com/2075-163X/7/3/34/s1, Figures S1–S17: Observed (dotted upper line), calculated (solid upper line), and difference (solid lower line) powder diffraction patterns of ZSM-5 at 30, 50, 75, 90, 125, 150, 175, 200, 225, 250, 300, 350, 400, 450, 500, 550 and 600 °C. Crystallographic data from the Rietveld refinement are also reported; Tables S1–S3: Fractional atomic coordinates of ZSM-5 loaded with MTBE at Room Temperature (30 °C), 100 and 400 °C.

Acknowledgments: Research co-funded by the Research Centre for Unconventional Energies, Istituto ENI G. Donegani-Environmental Technologies (San Donato Milanese (MI), Italy). Elisa Rodeghero, Annalisa Martucci and Giuseppe Cruciani also acknowledge MIUR for funding support within PRIN2010 programme (prot. 2010EARRRZ_009). We would like to acknowledge the also the European Synchrotron Radiation Facility (ESRF, Grenoble) for providing beam time (proposal CH-3510—In situ XRD study of structural modifications and desorption kinetics of zeolites used for removal of non-polar organic compounds from contaminated water).

Author Contributions: The manuscript was written with contributions from all authors. All authors have given approval to the final version of the manuscript. Elisa Rodeghero wrote the paper and performed the X-ray experiments with Giuseppe Cruciani; Luisa Pasti, Roberto Bagatin and Annalisa Martucci conceived and designed the experiments and analyzed the data.

Conflicts of Interest: The authors declare no conflict of interest.

References

1. Chong, M.N.; Jin, B.; Chow, C.W.; Saint, C. Recent developments in photocatalytic water treatment technology: A review. *Water Res.* **2010**, *44*, 2997–3027. [CrossRef] [PubMed]
2. Johnson, R.; Pankow, J.; Bender, D.; Price, C.; Zogorski, J. MTBE—To What Extent Will Past Releases Contaminate Community Water Supply Wells? *Environ. Sci. Technol.* **2000**, *34*, 210A–217A. [CrossRef] [PubMed]
3. Amberg, A.; Rosner, E.; Dekant, W. Toxicokinetics of methyl *tert*-butyl ether and its metabolites in humans after oral exposure. *Toxicol. Sci.* **2001**, *61*, 62–67. [CrossRef] [PubMed]
4. Mackay, D.; Shiu, W.Y.; Ma, K.C.; Lee, S.C. *Illustrated Handbook of Physical–Chemical Properties and Environmental Fate for Organic Chemicals—Volatile Organic Chemicals*; Taylor & Francis Group, LLC: Boca Raton, FL, USA, 2006; Volume 3, pp. 1–925.
5. Squillace, P.; Pankow, J.; Kortes, N.; Zogorski, J. Review of the environmental behavior and fate of methyl *tert*-butyl ether. *Environ. Toxicol. Chem.* **2009**, *16*, 1836–1844. [CrossRef]
6. United States Environmental Protection Agency. *Drinking Water Advisory: Consumer Acceptability Advice and Health Effects Analysis on Methyl Tertiary-Butyl Ether (MTBE)*; EPA-822-F-97-009; US Environmental Protection Agency: Washington, DC, USA, 1997; pp. 11–13.
7. Gaya, U.I.; Abdullah, A.H. Heterogeneous photocatalytic degradation of organic contaminants over titanium dioxide: A review of fundamentals, progress and problems. *J. Photochem. Photobiol. C Photochem. Rev.* **2008**, *9*, 1–12. [CrossRef]
8. Costa, A.A.; Wilson, W.B.; Wang, H.; Campiglia, A.D.; Dias, J.A.; Dias, S.C.L. Comparison of BEA, USY and ZSM-5 for the quantitative extraction of polycyclic aromatic hydrocarbons from water samples. *Microporous Mesoporous Mater.* **2012**, *149*, 186–192. [CrossRef]
9. Milestone, N.B.; Bibby, D.M. Concentration of alcohols by adsorption on silicalite. *J. Chem. Technol. Biotechnol.* **1981**, *31*, 732–736. [CrossRef]
10. Grose, R.W.; Flanigen, E.M. Novel Zeolite Compositions and Processes for Preparing and Using Same. U.S. Patent 4,257,885, 24 March 1981.
11. Yazaydin, A.O.; Thompson, R.W. Molecular simulation of the adsorption of MTBE in silicalite, mordenite, and zeolite beta. *J. Phys. Chem. B* **2006**, *110*, 14458–14462. [CrossRef] [PubMed]
12. Abu-Lail, L.; Bergendahl, J.A.; Thompson, R.W. Adsorption of methyl tertiary butyl ether on granular zeolites: Batch and column studies. *J. Hazard. Mater.* **2010**, *178*, 363–369. [CrossRef] [PubMed]
13. Anderson, M.A. Removal of MTBE and other organic contaminants from water by sorption to high silica zeolites. *Environ. Sci. Technol.* **2000**, *34*, 725–727. [CrossRef]
14. Rossner, A.; Knappe, D.R. MTBE adsorption on alternative adsorbents and packed bed adsorber performance. *Water Res.* **2008**, *42*, 2287–2299. [CrossRef] [PubMed]
15. Martucci, A.; Braschi, I.; Marchese, L.; Quartieri, S. Recent advances in clean-up strategies of waters polluted with sulfonamide antibiotics: A review of sorbents and related properties. *Mineral. Mag.* **2014**, *78*, 1115–1140. [CrossRef]
16. Braschi, I.; Blasioli, S.; Gigli, L.; Gessa, C.E.; Alberti, A.; Martucci, A. Removal of sulfonamide antibiotics from water: Evidence of adsorption into an organophilic zeolite Y by its structural modifications. *J. Hazard. Mater.* **2010**, *17*, 218–225. [CrossRef] [PubMed]
17. Martucci, A.; Pasti, L.; Marchetti, N.; Cavazzini, A.; Dondi, F.; Alberti, A. Adsorption of pharmaceuticals from aqueous solutions on synthetic zeolites. *Microporous Mesoporous Mater.* **2012**, *148*, 174–183. [CrossRef]
18. Pasti, L.; Martucci, A.; Nassi, M.; Cavazzini, A.; Alberti, A.; Bagatin, R. The role of water in DCE adsorption from aqueous solutions onto hydrophobic zeolites. *Microporous Mesoporous Mater.* **2012**, *160*, 182–193. [CrossRef]
19. Pasti, L.; Sarti, E.; Cavazzini, A.; Marchetti, N.; Dondi, F.; Martucci, A. Factors affecting drug adsorption on beta zeolites. *J. Sep. Sci.* **2013**, *36*, 1604–1611. [CrossRef] [PubMed]

20. Braschi, I.; Martucci, A.; Blasioli, S.; Mzini, L.L.; Ciavatta, C.; Cossi, M. Effect of humic monomers on the adsorption of sulfamethoxazole sulfonamide antibiotic into a high silica zeolite Y: An interdisciplinary study. *Chemosphere* **2016**, *155*, 444–452. [CrossRef] [PubMed]
21. Leardini, L.; Martucci, A.; Braschi, I.; Blasioli, S.; Quartieri, S. Regeneration of high-silica zeolites after sulfamethoxazole antibiotic adsorption: A combined in situ high-temperature synchrotron X-ray powder diffraction and thermal degradation study. *Mineral. Mag.* **2014**, *78*, 1141–1160. [CrossRef]
22. Grima, J.N.; Zammit, V.; Gatt, R.M. Negative Thermal Expansion. *Xjenza* **2006**, *11*, 17–29.
23. Bull, I.; Lightfoot, P.; Villaescusa, L.A.; Bull, L.M. An X-ray Diffraction and MAS NMR Study of the Thermal Expansion Properties of Calcined Siliceous Ferrierite. *J. Am. Chem. Soc.* **2003**, *125*, 4342–4349. [CrossRef] [PubMed]
24. Woodcock, D.A.; Lightfoot, P.; Wright, P.A.; Villaescusa, L.A.; Dìaz-Cabañasb, M.J.; Camblorb, M.A. Strong negative thermal expansion in the siliceous zeolites ITQ-1,ITQ-3 and SSZ-23. *J. Mater. Chem.* **1999**, *9*, 349–351. [CrossRef]
25. Alberti, A.; Martucci, A. Phase transformations and structural modifications induced by heating in microporous materials. *Stud. Surf. Sci. Catal.* **2005**, *155*, 19–43.
26. Alberti, A.; Martucci, A. Reconstructive phase transitions in microporous materials: Rules and factors affecting them. *Microporous Mesoporous Mater.* **2011**, *141*, 192–198. [CrossRef]
27. Cruciani, G. Zeolites upon heating: Factors governing their thermal stability and structural changes. *J. Phys. Chem. Solids* **2006**, *67*, 1973–1994. [CrossRef]
28. Leardini, L.; Martucci, A.; Alberti, A.; Cruciani, G. Template burning effects on stability and boron coordination in boron levyne studied by in situ time resolved synchrotron powder diffraction. *Microporous Mesoporous Mater.* **2013**, *167*, 117–126. [CrossRef]
29. Martucci, A.; Leardini, L.; Nassi, M.; Sarti, E.; Bagatin, R.; Pasti, L. Removal of emerging organic contaminants from aqueous systems: Adsorption and location of methyl-tertiary-butylether on synthetic ferrierite. *Mineral. Mag.* **2014**, *78*, 1161–1175. [CrossRef]
30. Arletti, R.; Martucci, A.; Alberti, A.; Pasti, L.; Nassi, M.; Bagatin, R. Location of MTBE and toluene in the channel system of the zeolite mordenite: Adsorption and host–guest interactions. *J. Solid State Chem.* **2012**, *194*, 135–142. [CrossRef]
31. Martucci, A.; Braschi, I.; Bisio, C.; Sarti, E.; Rodeghero, E.; Bagatin, R.; Pasti, L. Influence of water on the retention of methyl tertiary-butyl ether by high silica ZSM-5 and Y zeolites: A multidisciplinary study on the adsorption from liquid and gas phase. *RSC Adv.* **2015**, *5*, 86997–87006. [CrossRef]
32. Knappe, D.R.U.; Campos, A.A.R. Effectiveness of high-silica zeolites for the adsorption of methyl tertiary-butyl ether from natural water. *Water Sci. Technol. Water Supply* **2005**, *5*, 83–91.
33. Centi, G.; Grande, A.; Perathoner, S. Catalytic conversion of MTBE to biodegradable chemicals in contaminated water. *Catal. Today* **2002**, *75*, 69–76. [CrossRef]
34. Sacchetto, V.; Gatti, G.; Paul, G.; Braschi, I.; Berlier, G.; Cossi, M.; Bisio, C. The interactions of methyl *tert*-butyl ether on high silica zeolites: A combined experimental and computational study. *Phys. Chem. Chem. Phys.* **2013**, *15*, 13275–13287. [CrossRef] [PubMed]
35. Li, S.; Tuan, V.A.; Noble, R.D.; Falconer, J.L. MTBE adsorption on all-silica β zeolite. *Environ. Sci. Technol.* **2003**, *37*, 4007–4010. [CrossRef] [PubMed]
36. Baerlocher, C.; Meir, W.M.; Olson, O.H. *Atlas of Zeolite Framework Types*, 5th ed.; Elsevier Science: New York, NY, USA, 2001.
37. Larson, A.C.; von Dreele, R.B. *GSAS, General Structure Analysis System*; LANSCE, MS-H805; Los Alamos National Laboratory: Los Alamos, NM, USA, 1994.
38. Toby, B.H. EXPGUI, a graphical user interface for GSAS. *J. Appl. Crystallogr.* **2001**, *34*, 210–213. [CrossRef]
39. Martucci, A.; Pasti, L.; Nassi, M.; Alberti, A.; Arletti, R.; Bagatin, R.; Sticca, R. Adsorption mechanism of 1,2-dichloroethane into an organophilic zeolite mordenite: A combined diffractometric and gas chromatographic study. *Microporous Mesoporous Mater.* **2012**, *151*, 358–367. [CrossRef]
40. Degen, T.; Sadki, M.; Bron, E.; König, U.; Nénert, G. The HighScore suite. *Powder Diffr.* **2014**, *29*, S13–S18. [CrossRef]
41. Ardit, M.; Martucci, A.; Cruciani, G. Monoclinic–orthorhombic phase transition in ZSM-5 zeolite: Spontaneous strain variation and thermodynamic properties. *J. Phys. Chem. C* **2015**, *119*, 7351–7359. [CrossRef]

42. Martucci, A.; Rodeghero, E.; Pasti, L.; Bosi, V.; Cruciani, G. Adsorption of 1,2-dichloroethane on ZSM-5 and desorption dynamics by in situ synchrotron powder X-ray diffraction. *Microporous Mesoporous Mater.* **2015**, *215*, 175–182. [CrossRef]
43. Rodeghero, E.; Martucci, A.; Cruciani, G.; Bagatin, R.; Sarti, E.; Bosi, V.; Pasti, L. Kinetics and dynamic behaviour of toluene desorption from ZSM-5 using in situ high-temperature synchrotron powder X-ray diffractionand chromatographic techniques. *Catal. Today* **2016**, *227*, 118–125. [CrossRef]
44. Bhange, D.S.; Ramaswamy, V. High temperature thermal expansion behavior of silicalite-1 molecular sieve: In Situ HTXRD study. *Microporous Mesoporous Mater.* **2007**, *103*, 235–242. [CrossRef]
45. Bhange, D.S.; Ramaswamy, V. Enhanced negative thermal expansion in MFI molecular sieves by varying framework composition. *Microporous Mesoporous Mater.* **2010**, *130*, 322–326. [CrossRef]
46. Villaescusa, L.A.; Lightfoot, P.; Teat, S.J.; Morris, R.E. Variable-Temperature Microcrystal X-ray Diffraction Studies of Negative Thermal Expansion in the Pure Silica Zeolite IFR. *J. Am. Chem. Soc.* **2001**, *123*, 5453–5459. [CrossRef] [PubMed]
47. Milanesio, M.; Artioli, G.; Gualtieri, A.F.; Palin, L.; Lamberti, C. Template burning inside TS-1 and Fe-MFI molecular sieves: An in situ XRPD study. *J. Am. Chem. Soc.* **2003**, *125*, 14549–14558. [CrossRef] [PubMed]
48. Martucci, A.; de Lourdes Guzman-Castillo, M.; Di Renzo, F.; Fajula, F.; Alberti, A. Reversible channel deformation of zeolite omega during template degradation highlighted by in situ time-resolved synchrotron powder diffraction. *Microporous Mesoporous Mater.* **2007**, *104*, 257–268. [CrossRef]
49. Leardini, L.; Martucci, A.; Cruciani, G. The unusual thermal behaviour of boron-ZSM-5 probed by "in situ" time-resolved synchrotron powder diffraction. *Microporous Mesoporous Mater.* **2013**, *173*, 6–14. [CrossRef]
50. Leardini, L.; Martucci, A.; Cruciani, G. The unusual thermal expansion of pure silica sodalite probed by in situ time-resolved synchrotron powder diffraction. *Microporous Mesoporous Mater.* **2012**, *151*, 163–171. [CrossRef]
51. Leardini, L.; Quartieri, S.; Vezzalini, G.; Arletti, R. Thermal behaviour of siliceous faujasite: Further structural interpretation of negative thermal expansion. *Microporous Mesoporous Mater.* **2015**, *202*, 226–233. [CrossRef]